Real-Time 3-D Spatial-Temporal Dual-Polarized Measurement of Wideband Radio Channel at Mobile Station

Kimmo Kalliola, Heikki Laitinen, Leo I. Vaskelainen, and Pertti Vainikainen, *Member, IEEE*

***Abstract*—This paper describes a measurement system enabling the complete real-time characterization of the wideband radio channel. The system is based on a wideband radio channel sounder and a spherical antenna array, and it aims to describe the three-dimensional (3-D) spatial radio channel seen by the mobile terminal, including polarization. This information is highly valuable in designing antennas for mobile terminals. The spatial properties of the measurement system are analyzed through test measurements in an anechoic chamber. The system has a 40° spatial resolution and a 17 dB cross polarization discrimination. The values are well above those of a small mobile terminal antenna. The dynamic range in the spatial domain is 12 dB. The measurement is very fast, which makes real-time channel acquisition practical at normal mobile speeds.**

***Index Terms*—Conformal antennas, microstrip antennas, microwave measurements, mobile antennas, mobile communication, multipath channels, polarization, radio propagation.**

I. Introduction

THE demand for higher data rates sets high requirements for the future wireless mobile communication systems. Efficient use of the limited frequency spectrum requires thorough understanding of the wideband radio channel, also in the spatial domain. At the mobile terminal the spatial information can be exploited by matching the antenna properly to the radio environment, by correct design of both the power and polarization radiation patterns. The advantages are in lower transmission power and less radiation toward the user, which lead to increased battery lifetimes and lower interference levels in the networks. In addition, space and polarization diversity in reception are seen as applicable in mobile terminals operating in complex radio environments. The obtained diversity gain depends on the spatial properties of the radio channel.

Traditionally, mobile antennas have been evaluated based on their radiation properties, e.g., gain, measured in an anechoic chamber. However, the actual performance of a mobile handset antenna in a realistic operation environment depends on its mean effective gain (MEG) [1], which is the ratio of the power received by the antenna and the total mean incident power. In addition to the three-dimensional (3-D) radiation pattern of the antenna, MEG depends on the 3-D angular density functions of both the vertically polarized (VP) and horizontally polarized (HP) components of the incident waves in the environment, and on the cross polarization power ratio (XPR). These could be obtained through simulations, but the complexity of the operating environments makes the modeling of the spatial radio channel seen by the mobile very obscure. Particularly, the spatial channel models have to be extended to three dimensions at the mobile end, due to the scatterers close to the mobile e.g., inside buildings or in street canyons, that cause signal spreading in three dimensions.

Deterministic indoor channel models are usually based on ray-tracing or finite-difference time-domain (FDTD) methods [2]. The problem with those is that they are computationally complex, and also require a very detailed description of the particular environment, which makes the 3-D case even more difficult. Stochastic models for the spatial radio channel have also been developed [3], but there is a need for measurements to verify the models, and to adjust the parameters for different environments.

The 3-D angular density functions for the VP and HP signal components at the mobile station could be obtained by performing extensive measurement campaigns in realistic environments. Previously, the synthetic aperture measurement approach has been applied for 3-D radio channel measurements [4]. Also directional scanning with a narrow-beam antenna has been used [1], [5]. Both methods are, however, very slow and thus infeasible for collecting statistically significant amounts of data for directional signal distributions. In addition, they do not allow the characterization of the time-variant behavior of the channel (e.g., transients), and thus disable the verification of real dynamic channel models. Such would be needed for extensive evaluation of mobile terminal antennas in realistic operating environments.

A method for real-time spatial radio channel measurements has been presented in [6]. The method is based on using a complex wideband radio channel sounder together with a fast RF switch and an antenna array. The directions-of-arrival (DOA) of the incident waves can be estimated based on the relative phases of the array elements. So far the reported real-time spatial channel measurements have been limited to the azimuth domain [6], [7]. Typically these aim to describe the spatial radio

Manuscript received May 26, 1999; revised February 3, 2000. This work was supported by the Wihuri Foundation, Tekniikan edistämissäätiö, Academy of Finland, Technology Development Centre of Finland, Nokia, Sonera, and Finnet Group.

K. Kalliola is with Helsinki University of Technology, Radio Laboratory, FIN-02015 HUT, Finland, and with Nokia Research Center, FIN-00045 Nokia Group, Finland (e-mail: kimmo.kalliola@hut.fi; kimmo.kalliola@nokia.com).

H. Laitinen and L. I. Vaskelainen are with VTT Information Technology, Telecommunications, FIN-02044 VTT, Finland (e-mail: heikki.laitinen@vtt.fi; leo.vaskelainen@vtt.fi.).

P. Vainikainen is with Helsinki University of Technology, Radio Laboratory, FIN-02015 HUT, Finland (e-mail: pva@radio.hut.fi).

Publisher Item Identifier S 0018-9456(00)03584-1.

environment seen from a base station (BS) of a cellular system, where normally the elevation angles of incident waves do not vary significantly.

In this paper, we apply the same method for the real-time spatial channel measurement in the 3-D case of the mobile station. The measurement enables the complete real-time spatio-temporal characterization of the wideband mobile radio channel. The excess delay, azimuth angle, elevation angle, polarization state, amplitude, and phase of the multipath components of the transmitted signal can be measured. The fast measurement allows also the calculation of the Doppler spectrum of each wave. The 3-D spatial measurement is based on a dual-polarized spherical antenna array.

The measurement system is described, and two different approaches to resolve the spatial information are presented and compared in this paper. The directional properties of the measurement system including angular resolution, spatial dynamic range, cross polarization discrimination, accuracy of measured incidence angle, and amplitude and phase ripple versus incidence angle are defined with test measurements.

II. Description of Measurement System

The measurement system is based on a spherical array of 32 dual-polarized antenna elements and a complex wideband radio channel sounder [8]. A wideband signal is transmitted using a single antenna with linear polarization, and received separately with each of the 32 elements and both θ and ϕ polarizations, using a fast 64-channel RF switch. The carrier frequency of the sounder is 2.154 GHz, and the chip frequency of the modulating pseudo-random sequence in the transmitter can be selected to be up to 30 MHz, resulting in delay resolution of 33 ns. In the receiver, the demodulated signal is divided into I- and Q-branches and sampled with two 120 Msps A/D-converters. The signal samples from each branch of the switch are then stored for off-line processing to obtain the complex impulse response (IR) of the channel corresponding to each element and polarization.

A. Array Geometry

The ideal way to cover the whole 4π angle in space with direction-independent angular resolution would be to use equally spaced elements on the surface of a sphere. However, it is not possible to distribute any number of points on a sphere with each one equidistant from its neighbors. In other words, regular polyhedra exists only for certain numbers of vertices, and 32 is not one of them.

The geometry of the built array is based on the dual of the Archimedian solid, the truncated icosahedron, which is probably best known today as the geometry of the soccer ball. One element is located in each vertex of the polyhedron, and two different distances between adjacent elements exist. The nearest neighbors of an element are always at a distance of $0.641R$ and the next at $0.714R$ from the element, where R is the distance from the center of the structure to each element. Every element has either five or six such neighbors. It is shown in [9] that this arrangement minimizes the Coulombic potential of a system of 32 point charges distributed on the surface of a sphere, thus approximating an even distribution.

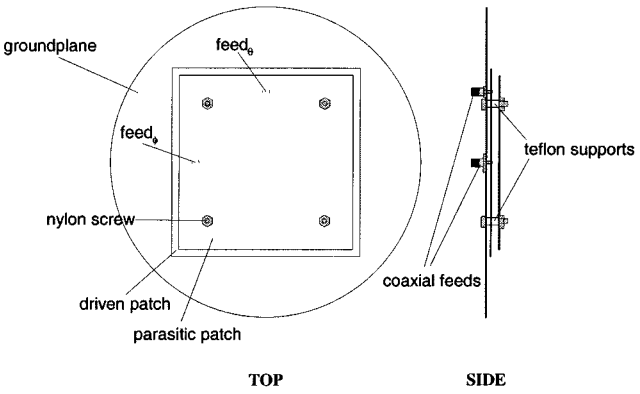

Fig. 1. Geometry of the microstrip patch element used in the spherical array.

B. Array Element

The main requirements for the element of the array are two separate feeds for orthogonal polarizations with high cross polarization discrimination (XPD), and sufficient bandwidth to meet the requirement of the measurement system. The used element is a stacked microstrip patch antenna with separate probe feeds for ϕ and θ polarizations [10]. The geometry of the antenna element is presented in Fig. 1. Fig. 2 presents the radiation pattern of the element, measured with all elements attached to the spherical array.

The 6-dB beamwidth of the element is 90° in the E-plane and 100° in the H-plane. The XPD is better than 18 dB within the 6-dB beamwidth. The measured gain of the element is 7.8 dBi. The return loss is over 10 dB inside the frequency band of the channel sounder (2154 ± 50 MHz).

C. Array Realization

The antenna elements are mounted on a spherical surface consisting of two hollow aluminum hemispheres with outer diameter of 330 mm (2.37 λ at 2.154 GHz). The elements are isolated from the mount, and the distance from the center of the driven patch (see Fig. 1) to the center of the sphere is 170 mm. The elements point toward the normal of the sphere, and they are oriented so that the polarization vectors corresponding to the feeds (ϕ and θ) are parallel to unit vectors $\mathbf{u}_\phi$ and $\mathbf{u}_\theta$, respectively. One of the elements is located in the zenith of the sphere, pointing at the positive z-axis direction. Fig. 3 presents the configuration of the spherical array.

To reduce cabling and losses, the 64-channel RF switching unit is placed inside the sphere together with its control electronics. Only the RF signal cable, two coaxial control cables, and the power supply wires are leading outside of the sphere, which minimizes the disturbance to the near field of the array. The diameter of the sphere (330 mm) is determined by the physical size of the switching unit, although a lower sidelobe level (directional dynamic range) could be obtained by a smaller diameter. The grating lobes (secondary maxima in radiation pattern), however, are not a problem in the spherical array, as in most array geometries when wide element spacing is used. As

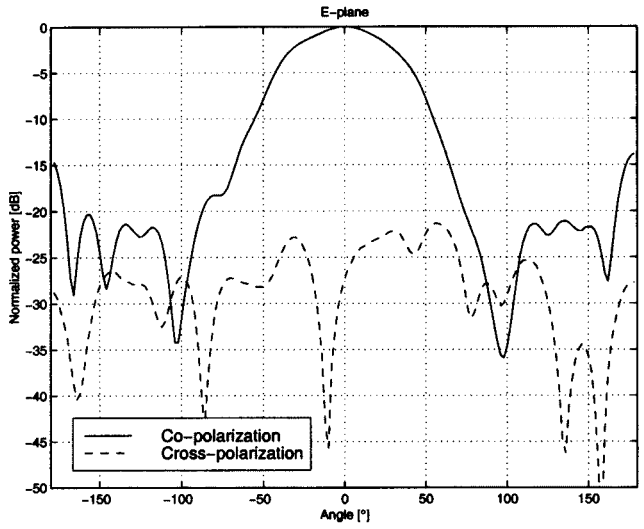

(a)

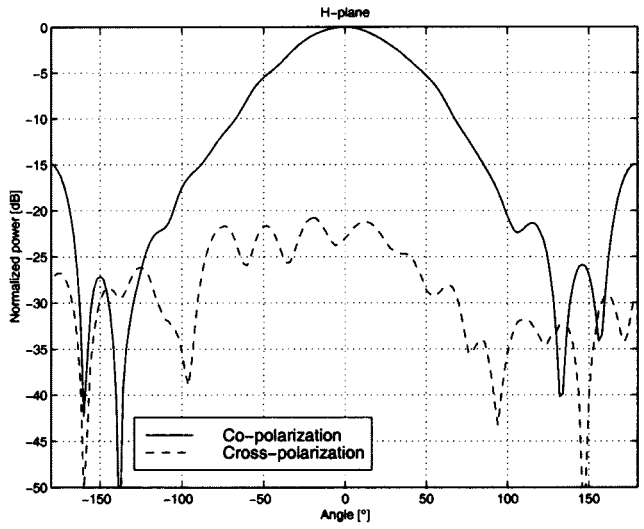

(b)

Fig. 2. Radiation pattern of antenna element measured with all elements attached to the spherical array. (a) E-plane. (b) H-plane.

calculated in [11], the grating lobe level of a spherical array is 27 dB below the main beam even with an element spacing of 1.0 λ. The average distance between adjacent elements in the built array is approximately 0.8 λ, and the directional element pattern further suppresses the grating lobe. Moreover, the mutual coupling between the elements is reduced with wider spacing. No mutual coupling compensation has been performed for the array.

III. Directional Measurement with Spherical Array

The far field of an arbitrary group of N dual-polarized antenna elements at direction (θ, ϕ) can be expressed as

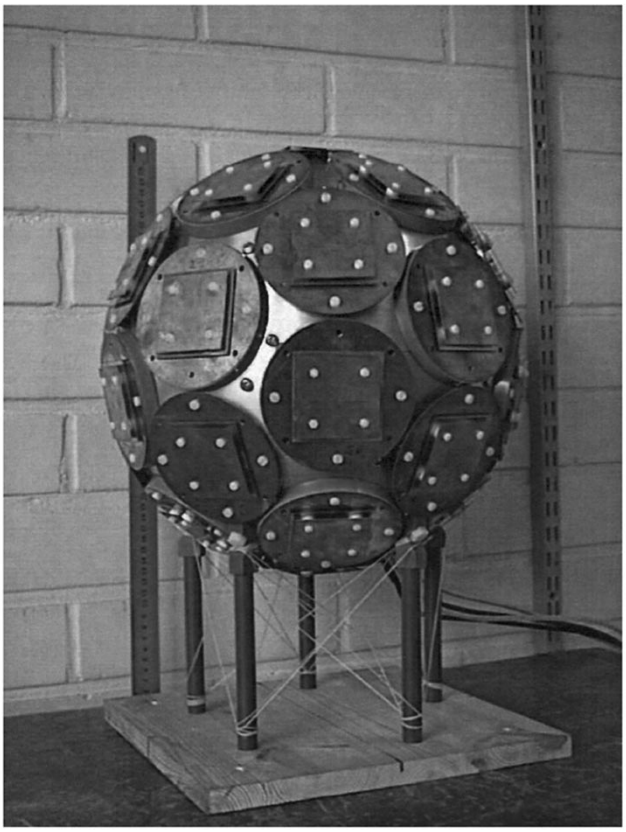

Fig. 3. Spherical array of 32 dual-polarized microstrip patch elements.

$$\begin{aligned}\mathbf{E}(\theta,\phi) &= q\sum_{n=1}^{N} w_n e^{j\frac{2\pi}{\lambda}\mathbf{r_n}\cdot\mathbf{u_r}(\theta,\phi)}\left[h_n \mathbf{g}_n^{\theta}(\theta,\phi)\right. \\ &\quad \left. + \nu_n \mathbf{g}_n^{\phi}(\theta,\phi)\right] \\ \mathbf{r_n} &= x_n\cdot\mathbf{u_x} + y_n\cdot\mathbf{u_y} + z_n\cdot\mathbf{u_z} \\ \mathbf{u_r}(\theta,\phi) &= \sin\theta\cos\phi\cdot\mathbf{u_x} + \sin\theta\sin\phi\cdot\mathbf{u_y} + \cos\theta\cdot\mathbf{u_z} \end{aligned} \quad (1)$$

where

q	array input signal;
w_n	complex weight of element n;
λ	carrier wavelength;
$\mathbf{r_n}$	position vector of element n;
θ	elevation angle from positive z-axis;
ϕ	azimuth angle CCW from positive x-axis (looking from positive z-axis direction);
$\mathbf{u_r}$	unit vector pointing at direction (θ, ϕ);
$\mathbf{g}_n^{\phi}(\theta,\phi)$	ϕ-polarized component of the field pattern of element n;
$\mathbf{g}_n^{\theta}(\theta,\phi)$	θ-polarized component of the field pattern of element n.

The element field pattern is defined by

$$\begin{aligned}\mathbf{g}_n^{\phi}(\theta,\phi) &= \mathbf{g}^{\phi}(\theta-\theta_n, \phi-\phi_n) \\ \mathbf{g}_n^{\theta}(\theta,\phi) &= \mathbf{g}^{\theta}(\theta-\theta_n, \phi-\phi_n)\end{aligned} \quad (2)$$

where θ_n and ϕ_n are the elevation and azimuth pointing directions of element n, respectively, and $\mathbf{g}^{\phi}$ and $\mathbf{g}^{\theta}$ are the measured element radiation patterns for the two polarizations. Coefficients

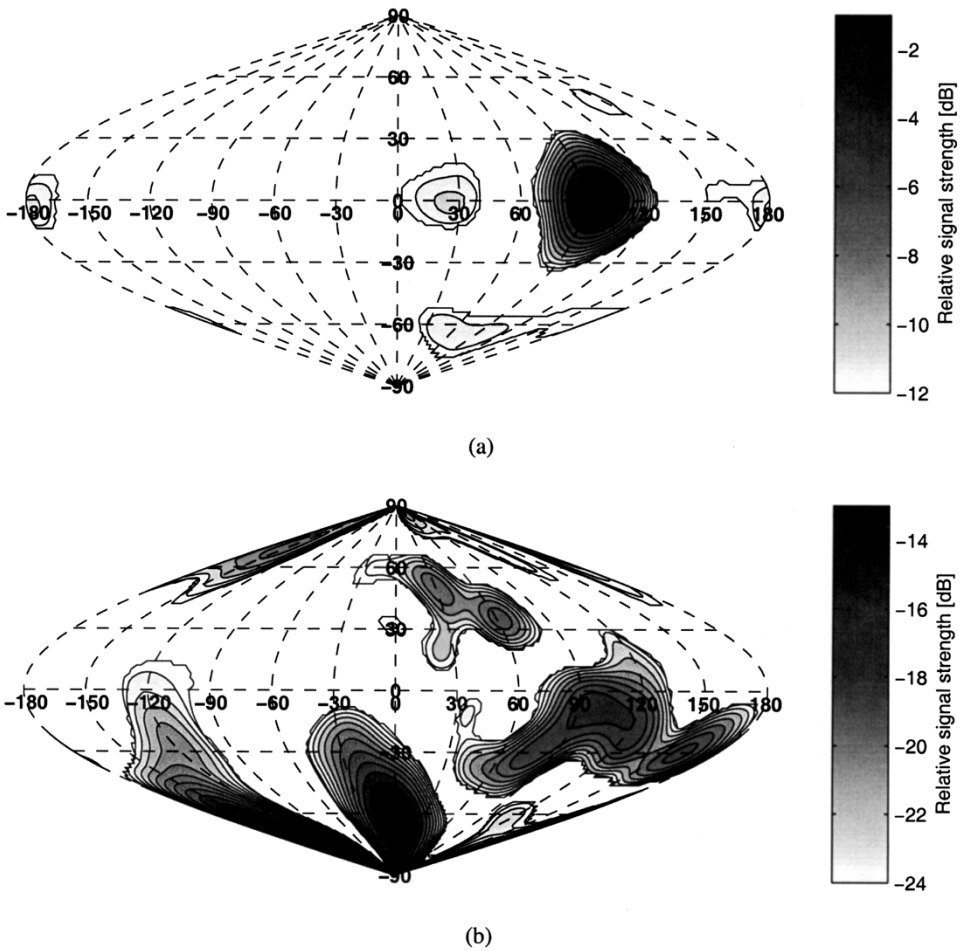

Fig. 4. Spatial response of the spherical array calculated with *element phasing* in the case of *one vertically polarized signal source* in direction $(+99°, 0°)$. (a) Vertical polarization. (b) Horizontal polarization.

h_n and v_n are applied to take into account the location-dependent orientation of the element polarization vectors, and are defined as

$$\begin{aligned} h_n &= \mathbf{p} \cdot \mathbf{u}_\phi(\theta_n, \phi_n) \\ &= \mathbf{p} \cdot (-\sin\phi_n \cdot \mathbf{u_x} + \cos\phi_n \cdot \mathbf{u_y}) \\ \nu_n &= \mathbf{p} \cdot \mathbf{u}_\theta(\theta_n, \phi_n) \\ &= \mathbf{p} \cdot (\cos\theta_n \cos\phi_n \cdot \mathbf{u_x} \\ &\quad + \cos\theta_n \sin\phi_n \cdot \mathbf{u_y} - \sin\theta \cdot \mathbf{u_z}) \end{aligned} \tag{3}$$

where $\mathbf{p}$ is the desired polarization vector, for which the field is to be calculated. In dual-polarized spatial channel measurements the two most practical values for vector $\mathbf{p}$ are the HP and VP components of the incident wave, namely, $\mathbf{u}_\phi(\theta, \phi)$ and $\mathbf{u}_\theta(\theta, \phi)$. In this case, the equations for h_n and v_n can be written as

$$\text{HP}: \quad \begin{cases} h_n = \mathbf{u}_\phi(\theta, \phi) \cdot \mathbf{u}_\phi(\theta_n, \phi_n) \\ \quad = \sin\phi \sin\phi_n + \cos\phi \cos\phi_n \\ \nu_n = \mathbf{u}_\phi(\theta, \phi) \cdot \mathbf{u}_\theta(\theta_n, \phi_n) \\ \quad = -\sin\phi \cos\theta_n \cos\phi_n \\ \qquad + \cos\phi \cos\theta_n \sin\phi_n \end{cases}$$

$$\text{VP}: \quad \begin{cases} h_n = \mathbf{u}_\theta(\theta, \phi) \cdot \mathbf{u}_\phi(\theta_n, \phi_n) \\ \quad = -\cos\theta \cos\phi \sin\phi_n \\ \qquad + \cos\theta \sin\phi \cos\phi_n \\ \nu_n = \mathbf{u}_\theta(\theta, \phi) \cdot \mathbf{u}_\theta(\theta_n, \phi_n) \\ \quad = \cos\theta \cos\phi \cos\theta_n \cos\phi_n \\ \qquad + \cos\theta \sin\phi \cos\theta_n \sin\phi_n \\ \qquad + \sin\theta \sin\theta_n . \end{cases} \tag{4}$$

The complex weights w_n can be used to form a beam toward a desired direction. The 3-D spatial response of the radio channel can be measured by forming a grid of beams covering the whole 4π solid angle. Two methods to determine the corresponding weight vectors are presented in the following.

A. Element Phasing

The simplest method to create a beam toward a certain direction (θ_0, ϕ_0) is to phase the element signals in that direction. In this case the weights are written as

$$w_n(\theta_0, \phi_0) = a_n(\theta_0, \phi_0) e^{-j\frac{2\pi}{\lambda}\mathbf{r_n} \cdot \mathbf{u_r}(\theta_0, \phi_0)} \tag{5}$$

where a_n is an amplitude tapering coefficient applied to suppress the array sidelobes.

If s_n and t_n are the signals measured from element n at two orthogonal polarizations (ϕ and θ), the spatial response becomes

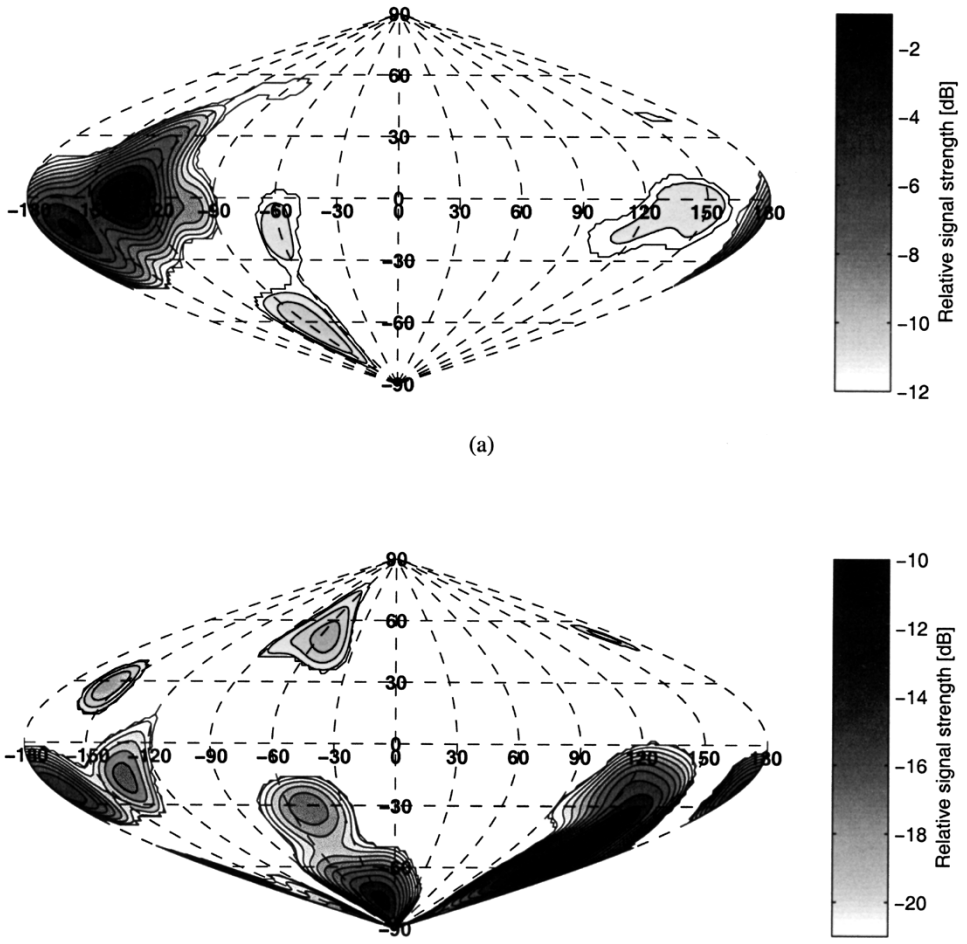

Fig. 5. Spatial response of the spherical array calculated with *element phasing* in the case of *two signal sources* in directions $(-128°, 0°)$ and $(-159°, -12°)$. (a) Vertical polarization. (b) Horizontal polarization.

$$S(\theta,\phi)=\sum_{n=1}^{N}[h_n(\theta,\phi)s_n+\nu_n(\theta,\phi)t_n]w_n(\theta,\phi) \qquad \begin{cases}\theta=0°\ldots180°\\ \phi=-180°\ldots+180°\end{cases} \tag{6}$$

which still has to be normalized to equalize the response for all directions. Let us assume a single plane wave with field vector $\mathbf{q}$ arriving at the array from direction (θ_s,ϕ_s). In this case signals s_n and t_n contain the direction-dependent phase information corresponding to the location of the element, and they are weighted by the element pattern at (θ_s,ϕ_s)

$$\begin{bmatrix}s_n\\ t_n\end{bmatrix}=e^{j\frac{2\pi}{\lambda}\mathbf{r_n}\cdot\mathbf{u_r}(\theta_s,\phi_s)}\begin{bmatrix}\mathbf{g}_n^{\phi}(\theta_s,\phi_s)\cdot\mathbf{q}\\ \mathbf{g}_n^{\theta}(\theta_s,\phi_s)\cdot\mathbf{q}\end{bmatrix}. \tag{7}$$

Substituting this for (6) and using element phasing from (5), gives

$$S(\theta,\phi)=\sum_{n=1}^{N}a_n(\theta,\phi)e^{-j\frac{2\pi}{\lambda}[\mathbf{r_n}\cdot\mathbf{u_r}(\theta,\phi)-\mathbf{r_n}\cdot\mathbf{u_r}(\theta_s,\phi_s)]}\cdot\left[h_n\mathbf{g}_n^{\phi}(\theta_s,\phi_s)\cdot\mathbf{q}+\nu_n\mathbf{g}_n^{\theta}(\theta_s,\phi_s)\cdot\mathbf{q}\right]. \tag{8}$$

It can be seen that the maximum of the response is produced toward direction $(\theta=\theta_s,\phi=\phi_s)$. The highest level is produced if the field vector $\mathbf{q}$ is matched to the desired polarization vector. The remaining part of the response is not zeros, but spurious responses whose level depends on the geometry of the array, and the amplitude tapering term a_n.

The tapering function that has been used for the spherical array is the normalized power function written as

$$a_n(\theta,\phi)=\left(\frac{R+\mathbf{r_n}\cdot\mathbf{u_r}(\theta,\phi)}{2R}\right)^P \tag{9}$$

where R is the radius of the sphere. The weight of the element pointing at the desired direction is unity while the element pointing at the opposite direction is nulled.

B. Beam Synthesis

In addition to simple phasing, the weight vector corresponding to a beam in a certain direction can be found through numeric beam synthesis. In the directional channel measurement approach this method can be applied to produce a weight vector that suppresses the spurious responses in the directional

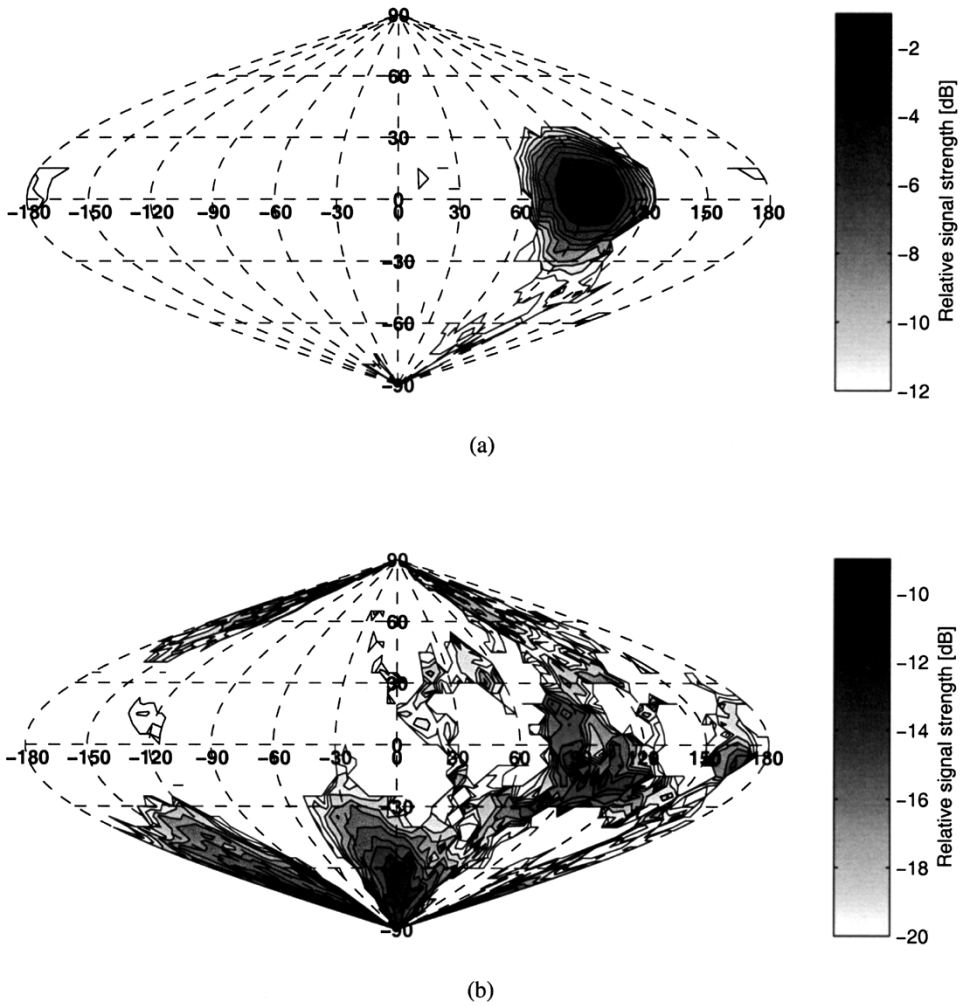

Fig. 6. Spatial response of the spherical array calculated with *beam synthesis* in the case of *one vertically polarized signal source* in direction $(+99°, 0°)$. (a) Vertical polarization. (b) Horizontal polarization.

response. A suitable beam synthesis method for conformal arrays is the iterative least-squares synthesis presented in [12].

The method is based on minimizing the difference between the radiation pattern and a given target function. To produce a grid of beams for directional scanning, one target function has to be defined for each discrete angle in the desired grid, as well as for both horizontal and vertical polarization.

The used target function has a rotationally symmetric beam with 3-dB beamwidth of 33°, and sidelobe level greater than -19 dB. The function was computed for a 5° angular grid, to ease the computational complexity.

The presented methods for calculating the spatial channel information are based on beam-scanning. Also more sophisticated super resolution algorithms could be used, that enhance the spatial properties of the measurement, but are more complex. Those are left out of the scope of this paper.

IV. Measurement System Analysis

A. Parameters Describing Directional Accuracy

The spatial dual-polarized channel measurement can be characterized by angular resolution and dynamic range, cross polarization discrimination, accuracy of measured incidence angle, and amplitude and phase ripple versus incidence angle. The angular resolution and dynamic range limit the measurement if the signal multipath components can not be separated in the delay domain. The achieved delay resolution for 30 MHz spreading code frequency is 33 ns corresponding to a 10 m difference in path length. Thus the dynamic range of the measurement is typically determined by the dynamic range of the measurement system in the delay domain, and is of the order of 30 dB. The temporal accuracy of the measurement system is described in [8].

1) Angular Resolution: In DOA estimation through beam-scanning the angular resolution is determined by the array beamwidth, and the used angular grid. A narrow beam and thus fine resolution is obtained with a large antenna aperture. The half-power beamwidth (HPBW) of a spherical array of isotropic elements and uniform illumination is approximately $50\ \lambda/D°$, where λ is the wavelength and D is the array diameter [11]. The angular resolution could be enhanced using more sophisticated algorithms than beam-scanning.

2) Spatial Dynamic Range: The dynamic range of the measurement in the spatial domain is limited by the sidelobe level

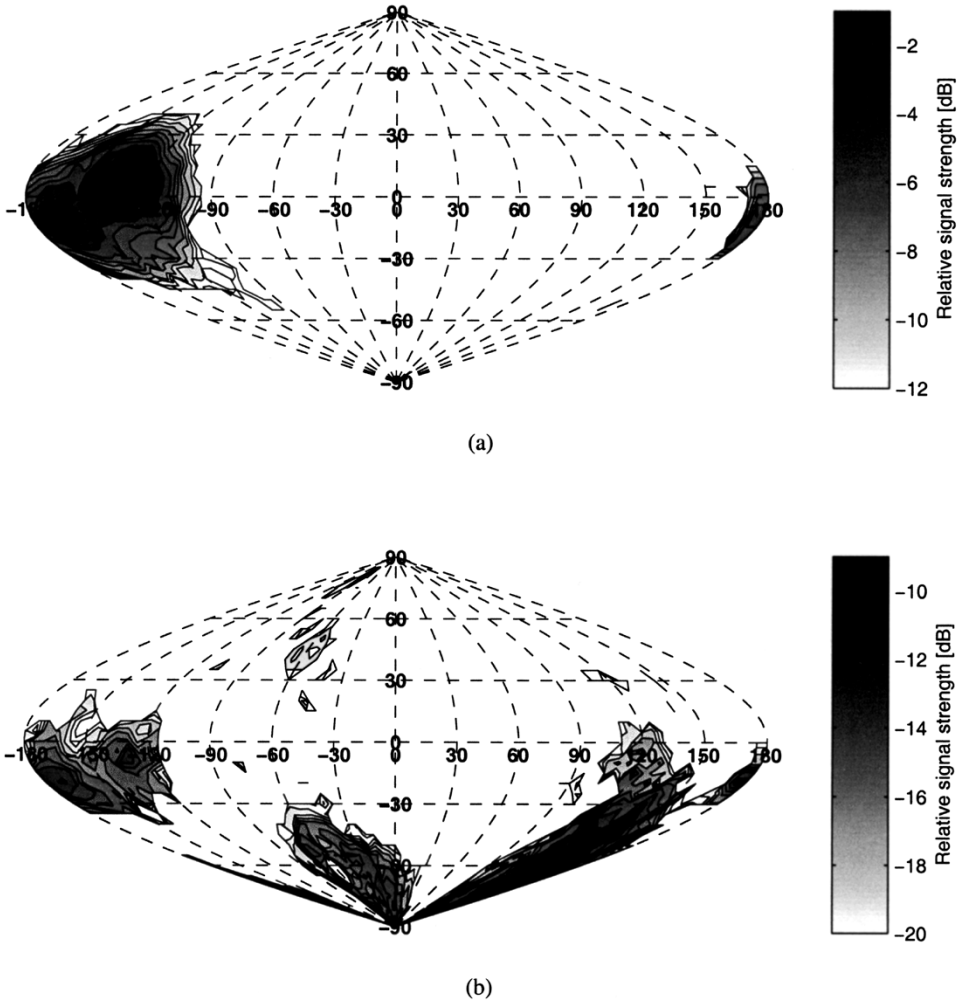

Fig. 7. Spatial response of the spherical array calculated with *beam synthesis* in the case of *two signal sources* in directions $(-128°, 0°)$ and $(-159°, -12°)$. (a) Vertical polarization. (b) Horizontal polarization.

of the array, since a strong signal at the direction of a sidelobe is interpreted as a weak signal at the main beam direction. The level of the highest sidelobes in a spherical array of isotropic elements and uniform illumination is -13 dB [11]. Amplitude tapering can be used to decrease the sidelobe level, but with a cost of increased beamwidth and decreased resolution.

3) Cross Polarization Discrimination: The polarizarion properties of the measurement can be described by the XPD, which is the ratio of the measured vertically and horizontally polarized signal components, in the case of a vertically polarized incident wave. In the case of conformal arrays with elements pointing at different directions, the XPD of the measurement is not determined solely by the XPD of the element, but also by the array geometry.

4) Accuracy of Measured Incidence Angle: The accuracy of the measured incidence angle of the wave depends on the accuracy of the measured phase of the element signal, according to (6). In the multiplexed case this is mainly determined by the mobile speed and the measurement rate [6], [13]. Also the finite angular grid in the beam-scanning process causes inaccuracy of the incidence angle.

5) Amplitude and Phase Ripple Versus Incidence Angle: Due to array imperfections (mutual coupling, unequal element patterns), the measured amplitude and phase vary as a function of the incidence angle of the signal. The effect could be reduced through a calibration procedure [14].

B. Accuracy Evaluation

The spatial properties of the measurement system have been studied by measuring the spatial impulse response of a known radio channel, using an anechoic chamber, which has a reflectivity level of -21 dB at the measurement frequency. In the anechoic chamber, the measured impulse response contains only one tap. The directional responses were calculated for that tap only. In measurements of realistic channels, the calculation is performed for each tap (multipath) separately. At first, one vertically polarized signal source was located at horizontal direction $(\theta = 90°)$. The spherical array was rotated 360° around the vertical axis and one impulse response was measured at 2° intervals from each antenna element (both polarizations). Thus, the spatial response of the array was measured for an azimuth range of $\phi = -180° \ldots +180°$ at an elevation angle of $\theta = 90°$. The result represents a worst case scenario, since the elements of the spherical array are positioned symmetrically above and below the equator of the sphere, and no elements point at the horizontal

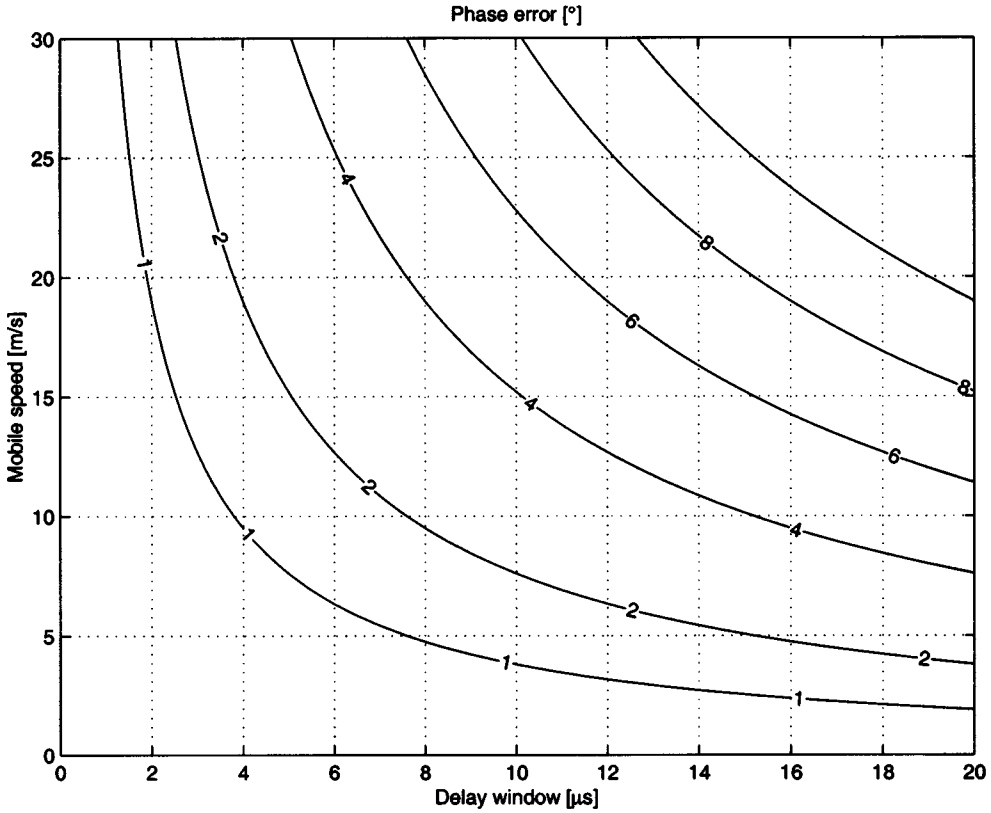

Fig. 8. Phase error between elements 1 and 32 caused by Doppler effect.

direction (see Fig. 3). The measurement was then repeated with an additional vertically polarized source at 12° below the horizontal plane and 31° apart the first source in the azimuth plane.

Figs. 4–7 show examples of the resulting normalized VP and HP spatial responses in both the one- and two-signal cases, and calculated for both methods: element phasing and numeric beam synthesis. Received power contours are shown with 1 dB intervals. Elevation angle 0° corresponds to the horizontal plane. In the element phasing case (Figs. 4 and 5) the directional response was calculated using (6) for an angular grid of 2°, with weights given in (5). Amplitude tapering coefficients from (9) were used with $p = 8$. In the beam synthesis case (Figs. 6 and 7) a sparse grid of 5° was used, resulting in a direction error, which can be seen as elevation offset from the horizontal plane in Fig. 6(a).

C. Phase and Direction Error due to Doppler Effect

The channel impulse responses are not measured exactly at the same time from all the antenna elements. Therefore, the Doppler effect causes phase rotation of the signal vectors between the elements [6], [13]. The phase error between the elements distorts the measured Doppler frequency of the incident waves. The maximum phase error between measuring the first and last array element is [6]

$$\Delta = 2 \cdot N \cdot \frac{\nu}{\lambda} \cdot \tau_{\max} \tag{10}$$

where N is the number of elements, ν is the radial speed of the mobile, and $\tau_{\max}$ is the delay window in the measurement (duration of the spreading code). Factor 2 is due to the two polarizations, that are measured subsequently from each element. The phase error given by (10) is shown in Fig. 8. It however presents the worst case, since the neighboring array elements are always measured subsequently, and the first and last elements look in different directions (straight up and straight down) and thus measure different waves. In the spherical array elements at three different elevation layers out of six measure the same signal. This eases the speed requirement by a factor of two.

The phase error caused by the Doppler effect also affects the measured incidence angles of the received signals. The effect has been studied by simulating the array response with the phasing method in the case of a plane wave source moving at speed ν. Fig. 9 presents the simulated DOA error as a function of mobile speed and delay window.

D. Summary of Accuracy

1) Directional Properties of Spherical Array: The 3-dB beamwidth of the spherical array is less than 40°, since the two sources with angular separation of approximately 40° [Figs. 4(a), 6(a)] can be separated at the −4 dB level. In Figs. 4(a)–7(a) it can also be observed that the sidelobe level in the one- (two-) signal case is −11 dB (−10 dB) for the phasing and −12 dB (−12 dB) for the numeric beam synthesis, respectively. In Figs. 4(b)–7(b) it is shown that the maxima in the cross-polarized responses are produced in other directions than the direction of the highest power, and can thus be considered as sidelobes. The XPD value in the true signal direction is always higher than these maxima.

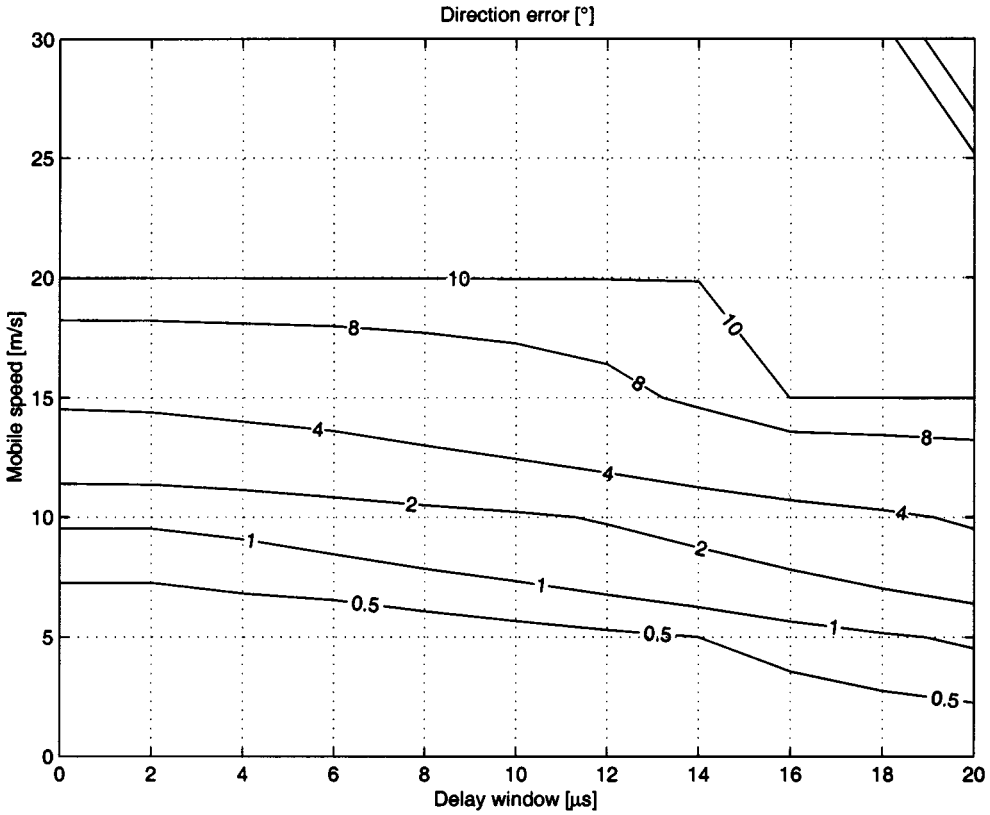

Fig. 9. Error in measured incidence angle caused by Doppler effect.

TABLE I
PARAMETERS DESCRIBING MEASUREMENT ACCURACY

Amplitude ripple	±0.8 dB p-p
Phase ripple	±7° p-p
Azimuth direction error	0.97° rms
Elevation direction error	0.71° rms
Mean XPD	17.3 dB
XPD ripple	±4 dB p-p

2) Measurement Accuracy as a Function of Signal Incidence Angle: The results of the array rotation measurement in the anechoic chamber were further processed using an algorithm that selects only the local maxima in the spatial power response (both VP and HP), and calculates the following parameters for each maxima using the phasing method: amplitude, phase, azimuth angle, elevation angle, VP/HP power ratio, and VP/HP phase difference. The procedure equals to the one that is used in the measurements of realistic radio channels. The parameter values describing the measurement accuracy in the one signal case are shown in Table I. The values show that the system can well describe the signal environment of a small mobile terminal antenna.

3) Sensitivity to Mobile Speed: In the worst case, a maximum phase error of 10° corresponds to a mobile speed of over 30 m/s with a 12 μs (4 km) delay window. In practice the requirement is even relaxed, due to the consecutive measurement of adjacent elements. Similarly, a maximum allowed direction error of 10° corresponds to a 20 m/s mobile speed for up to 14 μs delay window. Thus real-time measurements of the dynamic radio channel can be performed at normal mobile speeds.

V. CONCLUSION

This paper presents a method for directional 3-D real-time measurements of the wideband mobile radio channel. The measurement method enables the separation of signal multipath components with the same excess delay and Doppler shift as long as their angular separation is not less than 40°, and path loss difference more than 12 dB. The cross polarization discrimination is 17 dB, and the rms error of the incidence angle measurement is approximately 1°. The system can thus well describe the signal environment of a small mobile terminal antenna. The fast measurement enables real-time channel acquisition at normal mobile speeds, and thus allows the collection of statistically significant amounts of data, as well as the verification of time-variant spatial channel models.

The spatial properties of the measurement system were evaluated with two methods: simple phasing of elements, and numeric beam synthesis. The differences between the methods were found to be small. The beam synthesis method produces a slightly lower sidelobe level, but is more computationally complex, since the beams have to be synthesized separately for each angle in the chosen grid.

The 3-D spatial and polarization information of the radio channel seen by the mobile is highly valuable in the evaluation of antennas for mobile terminals in realistic operating environments. Spatial channel measurements are needed for the verification of stochastic and deterministic channel models including the spatial dimension. The measured channels can also be used directly for playback simulations.

ACKNOWLEDGMENT

The authors wish to thank J. Ollikainen and V. Voipio for helping in the design of the antenna element, and E. Kahra for the fine work in the mechanical design of the spherical array.

REFERENCES

[1] T. Taga, "Analysis for mean effective gain of mobile antennas in land mobile radio environments," *IEEE Trans. Veh. Technol.*, vol. 39, pp. 117–131, May 1990.

[2] K. A. Remley, A. Weisshaar, and H. R. Anderson, "A Comparative study of ray tracing and FDTD for indoor propagation modeling," in *Proc. 48th IEEE Annu. Vehicular Technology Conf.*, Ottawa, Ont., Canada, May 18–21, 1998, pp. 865–869.

[3] J. Fuhl, A. F. Molisch, and E. Bonek, "A unified channel model for mobile radio systems with smart antennas," *Proc. Inst. Elect. Eng., Radar, Sonar Navig.: Special Issue on Antenna Array Processing Techniques*, vol. 145, pp. 32–41, Feb. 1998.

[4] J. Fuhl, J.-P. Rossi, and E. Bonek, "High-resolution 3-D direction-of-arrival determination for urban mobile radio," *IEEE Trans. Antennas Propagat.*, vol. 45, pp. 672–682, Apr. 1998.

[5] J. Ø Nielsen, G. F. Pedersen, and K. Olesen, "Computation of mean effective gain from 3-D measurements," in *Proc. 48th IEEE Annu. Vehicular Technology Conf.*, Houston, TX, May 16–20, 1999, pp. 787–791.

[6] K. Kalliola and P. Vainikainen, "Dynamic wideband measurement of mobile radio channel with adaptive antennas," in *Proc. 48th IEEE Annu. Vehicular Technology Conf.*, Ottawa, Ont., Canada, May 18–21, 1998, pp. 21–25.

[7] K. I. Pedersen, P. E. Mogensen, and B. H. Fleury, "Spatial channel characteristics in outdoor environments and their impact on BS antenna system performance," in *Proc. 48th IEEE Annu. Vehicular Technology Conf.*, Ottawa, Ont., Canada, May 18–21, 1998, pp. 719–723.

[8] J. Kivinen, T. Korhonen, P. Aikio, R. Gruber, P. Vainikainen, and S.-G. Häggman, "Wideband radio channel measurement system at 2 GHz," *IEEE Trans. Instrum. Meas.*, vol. 48, pp. 39–44, Feb. 1999.

[9] J. R. Edmundson, "The distribution of point charges on the surface of a sphere," *Acta Crystallogr. A, Found. Crystallogr.*, vol. 48, pp. 60–69, 1992.

[10] V. Voipio, "Wideband Patch Antenna Array Techniques for Mobile Communications," Licentiate thesis, Helsinki Univ. of Technology, Helsinki, Finland, Nov. 23, 1998.

[11] H. E. Schrank, "Basic theoretical aspects of spherical phased arrays," in *Phased Array Antennas, Proc. 1970 Phased Array Antenna Symp.*, A. Oliner and G. Knittel, Eds. Norwell, MA: Artech House, 1972.

[12] L. I. Vaskelainen, "Iterative least-squares synthesis methods for conformal array antennas with optimized polarization and frequency properties," *IEEE Trans. Antennas Propagat.*, vol. 45, pp. 1179–1185, July 1997.

[13] U. Trautwein, K. Blau, D. Brückner, F. Herrmann, A. Richter, G. Sommerkorn, and R. S. Thomä, "Radio channel measurement for realistic simulation of adaptive antenna arrays," in *2nd European Personal Mobile Radio Conf.*, Bonn, Germany, Sept. 30–Oct. 2 1997, pp. 491–498.

[14] R. S. Thomä, D. Hampicke, A. Richter, G. Sommerkorn, A. Schneider, and U. Trautwein, "Identification of time-variant directional mobile radio channels," in *Proc. 16th IEEE Instrum. Meas. Technol. Conf.*, Venice, Italy, May 24–26, 1999, pp. 176–181.

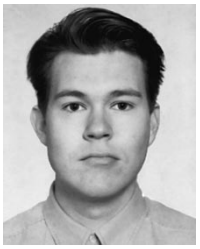

Kimmo Kalliola was born in Helsinki, Finland, in 1972. He received the M.S. degree in technology in 1997 from Helsinki University of Technology (HUT), Finland, where he is currently pursuing the Ph.D. degree in technology.

Since 1997, he has been with the Radio Laboratory of HUT as a Researcher. Since 1999, he has been also with Nokia Research Center, Finland. His research interests are in spatial radio channel measurements and urban radio propagation mechanisms.

Heikki Laitinen was born in Helsinki, Finland, in 1972. He received the M.S. degree in technology in 1999 from Helsinki University of Technology (HUT), Finland.

From 1994 to 1998, he was a Teaching Assistant at the Institute of Mathematics at HUT. Since 1998 he has been with the Technical Research Centre of Finland (VTT), where he is currently working as a Research Scientist in Wireless Systems research group. His present fields of interests include mobile radio propagation and channel modeling.

Leo I. Vaskelainen was born in Pieksämäki, Finland, in 1944. He received the degree of Diploma Engineer from Helsinki University of Technology, Espoo, Finland, in 1971.

He is currently a Senior Research Engineer in Technical Research Centre of Finland (VTT), Information Technology, Espoo, where he is responsible for research, design, and development of antenna analysis and synthesis, mobile communication systems, and radar systems. From 1970 to 1975, he was an Assistant in Helsinki University of Technology, Radiolaboratory. From 1975 to 1994, he worked at VTT Telecommunications Laboratory as Research Engineer, Senior Research Engineer, and as Section Leader of the Radio Section with responsibilites including research of nuclear electromagnetic pulse (NEMP), electromagnetic compatibility of electrical equipment, antenna techniques, microwave techniques, and radar techniques.

Pertti Vainikainen (M'91) was born in Helsinki, Finland, in 1957. He received the M.S. degree in technology, the Licentiate of Science degree in technology, and the Doctor of Science degree in technology from Helsinki University of Technology (HUT) in 1982, 1989, and 1991, respectively.

He was with the Radio Laboratory of HUT from 1981 to 1992, mainly as a Teaching Assistant and Researcher. From 1992 to 1993, he was Acting Professor of Radio Engineering, since 1993 Associate Professor of Radio Engineering, and since 1998, Professor in Radio Engineering, all at the Radio Laboratory of HUT. From 1993 to 1997, he was the Director of the Institute of Radio Communications (IRC) of HUT. His main fields of interest are RF techniques in radio communications and industrial measurement applications of radio waves. He is the author or coauthor of two books and about 80 refereed international journal or conference publications, and the holder of four patents.